Experiment and Theory of Fuel Cell Catalysis: Methanol and Formic Acid Decomposition on Nanoparticle Pt/Ru

ARTICLE *in* THE JOURNAL OF PHYSICAL CHEMISTRY C · SEPTEMBER 2008

Impact Factor: 4.77 · DOI: 10.1021/jp805374p

8 AUTHORS, INCLUDING:

wei-ping Zhou

32 PUBLICATIONS **1,700** CITATIONS

SEE PROFILE

Adam Lewera

University of Warsaw

44 PUBLICATIONS **1,128** CITATIONS

SEE PROFILE

Experiment and Theory of Fuel Cell Catalysis: Methanol and Formic Acid Decomposition on Nanoparticle Pt/Ru

Matthew A. Rigsby,[†] Wei-Ping Zhou,[†,⊥] Adam Lewera,[‡] Hung T. Duong,[†] Paul S. Bagus,[§] Wolfram Jaegermann,[∥] Ralf Hunger,[∥] and Andrzej Wieckowski*[,†]

Department of Chemistry, University of Illinois at Urbana−Champaign, Urbana, Illinois 61801, Department of Chemistry, University of Warsaw, ul. Pasteura 1, 02-093 Warsaw, Poland, Department of Chemistry, University of North Texas, Denton, Texas 76203-5070, and Surface Science Division, Institute of Materials Science, Darmstadt University of Technology, D-64287 Darmstadt, and Bessy-II, Berlin, Germany

Received: June 18, 2008; Revised Manuscript Received: July 29, 2008

This study seeks to explore the effects of the electronic structure of Pt/Ru alloy nanoparticles on reactivity of small organic molecules of relevance to fuel cell applications through the combined use of synchrotron radiation photoelectron spectroscopy and electrochemistry. Platinum core-level binding energies were found to increase linearly with the addition of ruthenium. This effect is a product of lattice strain and charge transfer, and is explained in terms of the d-band center theory proposed by Nørskov and co-workers (Hammer, B.; Nørskov, J. K. *Surf. Sci.* **1995**, *343*, 211). In the course of the study of electrooxidation of methanol we have found that it is very difficult, if not impossible, to separate the effects of the bifunctional mechanism and the electronic structure effects that might play a role in the activity. However, data for electrooxidation of formic acid, when studied at a short reaction time (where the indirect reaction pathways and poisoning intermediates are assumed to play a negligible role), demonstrate a definitive contribution from electronic structure on the reactivity. The reactivity of the Pt/Ru nanoparticles toward formic acid electrooxidation is discussed in terms of the d-band center theory.

1. Introduction

As a result of motivating factors such as cost, increasing energy demand, and environmental concerns, there is much interest in developing fuel cell technology, which has the potential to provide a cleaner and cheaper source of power. Direct liquid fuel cells, using methanol, ethanol, or formic acid, could be used as replacements for power sources in cell phones or laptop computers.[1−7] However, the high cost of platinum catalysts, slow reaction kinetics, poor selectivity, and catalyst poisoning have so far precluded the widespread use of fuel cells. Various bimetallic anode catalysts have been studied over the years in an effort to eliminate or reduce the negative effects of these issues. While not providing much benefit in terms of cost, Pt/Ru[8] has been shown to be effective in regards to the other factors, and is therefore one of the most commonly studied anode catalysts.

It is generally accepted that in bimetallic catalysts, enhancement of catalytic activity, as compared to monometallic catalysts, can be attributed to a bifunctional mechanism[9,10] and/or an electronic effect.[11,12] Via enhanced oxidation, the bifunctional mechanism of bimetallic catalysts assists in the removal of surface poisoning species, such as carbon monoxide, with each metal in the alloy playing a separate role. The effects of the electronic structure, on the other hand, are still not completely understood. A fundamental insight, including theoretical understanding of these mechanisms is necessary in order to design novel catalysts that can be used in new fuel cells. The density functional theory approaches developed by Nørskov et al.[13−20] have, for instance, indicated that changes in adsorption energies and activation barriers for reaction are directly linked to changes in position of the center of the metal/alloy d-band with respect to the Fermi level. The strength of binding of an atom or molecule to a surface depends on the degree of filling of the antibonding states between the two interacting species, and this, in turn, is dependent on the density of metal d states near the Fermi level. Consequently, one would expect to be able to tune the activity of a catalyst by inducing changes in its surface electronic structure. In an alloy, the surface electronic structure is affected by lattice strain[12,21−23] and charge transfer.[24] According to Nørskov's d-band center theory, these effects lead to narrowing or widening of the d-band and a subsequent shift in its center of gravity toward or away from the Fermi level to conserve energy and maintain a constant filling of the d-band. Conveniently, these shifts in the position of the center of the d-band are linked to shifts in core-level binding energies, making it possible to use core-level photoelectron spectroscopy to observe changes in surface electronic structure.[15,25−27]

There has been much effort to verify the d-band center theory through experimental techniques. While the theory has been found to not hold for some systems,[28] there have been major successes in connecting changes in adsorption to changes in position of the center of the d-band. One such example is the oxidation (desorption) of surface CO, which could be a useful measure of catalytic activity. In the study of Pt/Ru nanoparticles containing CO, Tong et al.[29] found that the addition of ruthenium to platinum led to a decrease in the local density of states of platinum. This change in electronic structure, due to the addition of ruthenium, reduces the $2\pi^*$ back-donation, and thereby

* To whom correspondence should be addressed. E-mail: andrzej@scs.uiuc.edu.
[†] University of Illinois at Urbana−Champaign.
[‡] University of Warsaw.
[§] University of North Texas.
[∥] Darmstadt University of Technology and Bessy-II.
[⊥] Present address: Chemistry Department, Brookhaven National Laboratory, Upton, NY, 11973.

10.1021/jp805374p CCC: $40.75
Published on Web 09/05/2008

weakens the metal−CO bond. Since CO is an important poisoning reaction intermediate in the oxidation of small organic molecules, this has major implications for catalytic oxidation of fuels like methanol and formic acid. In fact, Lu et al.[30,31] have demonstrated that the electronic (or ligand) effect has a definite contribution to the total enhancement of CO oxidation on Pt/Ru as compared to pure Pt, although the contribution is only about one-fourth that of the bifunctional mechanism. Recently, Alayoglu et al.[32] synthesized a ruthenium core-platinum shell nanoparticle catalyst based on first principles. This catalyst had low light-off temperatures for both CO and H_2, demonstrating a direct correlation between the electronic structure and activity in the gas-phase, as predicted by theory. However, despite the large amount of work,[33−39] the relationship between surface electronic structure and catalytic activity toward the electrooxidation of small organic fuels is not completely understood.

In this study, a series of Pt/Ru nanoparticles (produced by Johnson and Matthey), ranging in nominal composition from 0 to 100 atomic % Ru, were analyzed by synchrotron radiation photoelectron spectroscopy (SRPS) and chronoamperometry in an effort to determine whether a correlation between the d-band center theory and reactivity toward methanol and formic acid electrooxidation exists, and if it can be observed experimentally. It is generally accepted that, for sufficiently positive potentials, methanol electrooxidation on Pt/Ru alloys proceeds through a dual-pathway mechanism involving a strongly adsorbing CO intermediate.[9,10,40] Thus, although the electronic effect is believed to have some effect on the reactivity, the bifunctional mechanism, where Ru sites provide adsorbed oxygen-containing species for enhanced oxidative removal of adsorbed CO, is expected to play a larger role in the electrooxidation of methanol. On the other hand, formic acid is oxidized through a triple-pathway mechanism, where, at short reaction times and potentials below ~0.6 V vs RHE, a direct pathway to CO_2 formation dominates.[33,41,42] Under these conditions, where strongly adsorbed CO should play a negligible role, it may be possible to examine the effects of the bifunctional mechanism and the surface electronic structure separately, and thus to gain a better understanding of the processes involved.

2. Experimental Methods

The unsupported nanoparticle samples used in this study were obtained from Johnson and Matthey, and included the following. Pt black, Pt90Ru10, Pt80Ru20, Pt67Ru33, Pt50Ru50, Pt40Ru60, Pt34Ru66, and Ru black (where numbers indicate atomic % of the elements in the sample). For reactivity measurements, the nanoparticles were dispersed in Milli-Q water (18.2 MΩ), sonicated for 30 min, and deposited (~20 μL of an ~100 μg/mL solution) onto a gold disk (10 mm in diameter).[38] A thin film of nanoparticles over the entire disk was obtained after drying. The measurements were done in a conventional three-electrode cell with a platinum gauze counter electrode, Ag/AgCl (3 M NaCl, Bioanalytical Systems) reference electrode, and 0.5 M H_2SO_4 (GFS, doubly distilled from Vycor) electrolyte solution. Reactivity measurements were done in either 0.5 M CH_3OH/0.5 M H_2SO_4 or 0.2 M HCOOH/0.5 M H_2SO_4. For formic acid experiments, the current density was sampled at reaction times of 3 s and 1 h (then, under apparent steady-state), while for methanol experiments, only the steady-state current (at 1 h) was recorded. Methanol was purchased from Sigma-Aldrich and double distilled formic acid was purchased from GFS. Ultrahigh-purity (UHP) argon and carbon monoxide gases were provided by S. J. Smith Welding Supply. The catalyst surface area was calculated from CO stripping experiments, assuming a stripping charge of 420 μC cm^{-2}.[43] All samples were fully reduced by holding the electrode potential at −100 mV vs RHE for 2 h.[38]

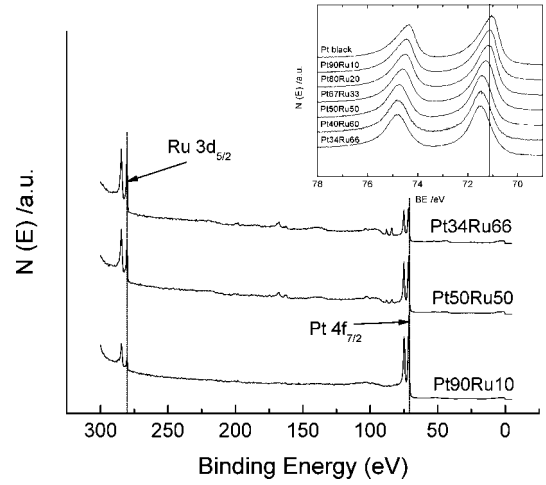

Figure 1. Typical wide-range survey spectra for three of the Pt/Ru nanoparticle samples recorded at Bessy-II ($h\nu$ = 370 eV). The inset shows the Pt 4f region of the spectra for all samples (increasing Ru from top to bottom). The vertical line marks the binding energy of pure Pt(111) as a reference.

The composition of the nanoparticles was verified and the core-level binding energies were measured using photoelectron spectroscopy at a synchrotron source (SRPS). These SRPS measurements[44] were obtained at Bessy-II in Berlin, using the undulator beamline U49/2-PGM 2 at the SoLiAS end station at photon energies of 160, 370, and 650 eV. The standard error for core-level binding energies at the synchrotron was 0.03 eV. The Au 4f signal from the Au substrate electrodes (10 mm in diameter) was kept at a negligible level (below 5 atomic %, as compared to the sum of Ru and Pt, see Figure 1). The instrumental and experimental details for the synchrotron measurements were reported previously.[44]

Structural and size properties were determined from powder X-ray diffraction (XRD) and high-resolution transmission electron microscopy (HRTEM, JEOL 2010F). XRD showed characteristic peaks for bulk Pt/Ru alloy, while no peaks for Ru oxides were observed. XRD and HRTEM gave similar particle size results (Table 1).

3. Results and Discussion

3.1. Synchrotron Radiation Photoelectron Spectroscopy of Pt/Ru Nanoparticles. Prior to recording core-level binding energies for the nanoparticle catalysts, the samples were all electrochemically pretreated as described in the Experimental Methods section. This pretreatment ensured an oxide-free surface, as confirmed by the synchrotron measurements. The typical wide-range survey spectra of the Ru/Pt samples are shown in Figure 1. Core-level binding energies of these samples (shown in Figure 1 inset) were reported previously[44] and are used here for further treatment. From Figure 1, there is a definite shift in the platinum core-level binding energy with changing composition. To demonstrate this more quantitatively, Figure 2 shows the relationship between Pt $4f_{7/2}$ binding energy and Ru content of the catalysts measured at photon energies of 160, 370, and 650 eV, where the Pt $4f_{7/2}$ binding energy increases linearly with increasing Ru content, with a slope of about 0.07 eV per 10% Ru. We have observed that the positive shift in the Pt 4f binding energy corresponds to a shift of the center of the

TABLE 1: Physical Characterization of Pt/Ru Nanoparticles

nominal Ru atomic %	crystalline size (nm)	lattice parameter (Å)	surface Ru atomic % from SRPS	Pt $4f_{7/2}$ BE (eV) ($h\nu$ = 160 eV)	catalyst surface area from CO stripping (cm^2)
0	8.0 ± 0.5	3.921	0	71.06	0.6 ± 0.1
10	8.8 ± 1.0	3.917	12	71.08	0.6 ± 0.1
20	5.5 ± 1.2	3.909	17	71.17	0.5 ± 0.1
33	4.4 ± 1.0	3.904	18	71.27	0.7 ± 0.1
50	3.1 ± 0.6	3.885	28	71.41	1.0 ± 0.2
60	3.0 ± 0.4	3.878	38	71.45	0.86 ± 0.07
66	3.0 ± 0.6	–	37	71.46	1.0 ± 0.2

d-band[15,25−27,36,45] toward higher binding energy, away from the Fermi level. As previously discussed, such a shift in the d-band center can be brought about by lattice strain and charge transfer. Our theoretical studies, which were previously reported,[44] indicate that the primary source of the shifts in core-level binding energies for the nanoparticles is lattice strain. This is in contrast to the results of a study of Pt single crystals, where the core-level shifts were clearly due to both lattice strain and charge transfer.[46] A change in the Pt−Pt bond distance with increasing alloyed Ru was confirmed by powder XRD, and the results are given in Table 1. As Ru is added to the alloy, the Pt lattice undergoes compressive strain, shortening the Pt−Pt bonds. This shortening of bond distances causes the d orbitals to overlap to a larger degree. Since the d-band of Pt is more than half-filled, broadening the d-band would be expected to lead to a subsequent downshift in the center of gravity of the d-band with respect to the Fermi level in order to maintain constant filling and to conserve energy. This is, in fact, what is observed through the core-level binding energy measurements.

The SRPS data was also used to determine the approximate surface composition of the nanoparticle catalysts based on the ratio of peak intensities of Pt $4f_{7/2}$ and Ru $3d_{5/2}$. Since the apparent surface composition calculated from SRPS depends on the photon energy used,[47] it was important to try to minimize the photon energy while matching the inelastic mean free paths for the two metals.[36] Both Pt 4f and Ru 3d core electrons have a kinetic energy of about 90 eV when Pt is measured with photon energy of 160 eV and Ru with 370 eV. The inelastic mean free path under this condition is ca. 4.2 Å,[47,48] which means that the SRPS signal is characteristic of predominantly the surface atoms. The surface composition of each catalyst was calculated using these photon energies, and the results are listed in Table 1. These data indicate an enrichment of Pt at the surface of the nanoparticles, which is in agreement with previous results by Babu et al.[49] using EC-NMR. It is likely that the Pt enrichment is a consequence of the strongly reducing environment that the samples are subjected to just prior to all experiments.[50,51]

3.2. Methanol Electrooxidation on Pt/Ru Nanoparticles. Decomposition of methanol on Pt results in a strong poisoning of surface Pt sites by carbon monoxide, and the oxidative removal of this CO requires the presence of a surface oxygen-containing species, as discussed above (the bifunctional mechanism). The enhancement provided by Ru is due to the ease with which water is activated over Ru, as compared to Pt, to form adsorbed oxygen-containing species.[8,9,40] In this work, the activity of the Pt/Ru nanoparticle catalysts toward electrooxidation of methanol was investigated by chronoamperometry. Figure 3 shows the current−time curves for methanol electrooxidation at 450 mV vs RHE for the different nanoparticle samples. There are two important features of these curves that should be noted. First, it is clear that the reactivity depends on the catalyst composition, as the current density is different for each sample at a given time. Second, the reactivity decreases over time until an apparent steady-state current is reached (at ca. 1 h). This decrease in reactivity is evidence of the poisoning effect, presumably of adsorbed CO formed as an intermediate in methanol electrooxidation.[40,52] In Figure 4, the steady-state current density is plotted as a function of Ru content. The obtained graph is a typical volcano plot,[53,54] where the current density is found to peak at a nominal composition of about

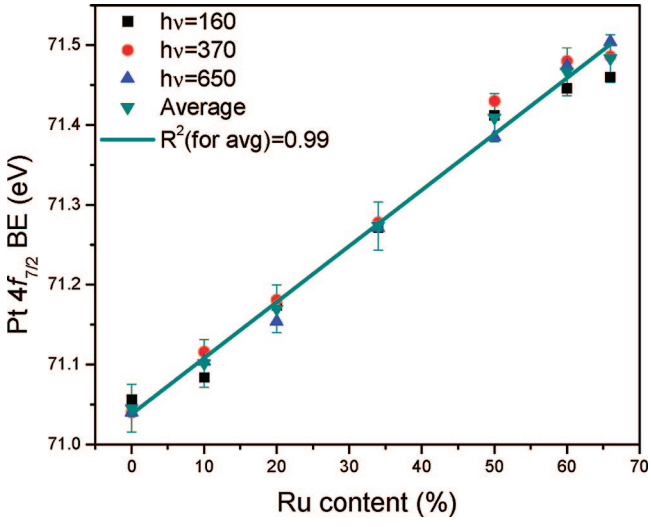

Figure 2. Pt $4f_{7/2}$ binding energy determined from synchrotron radiation experiments at Bessy-II ($h\nu$ = 160, 370, and 650 eV) as a function of Ru content in Pt/Ru nanoparticles. The linear fit is for the average binding energy for the three photon energies. The standard error was 0.03 eV for each measurement.

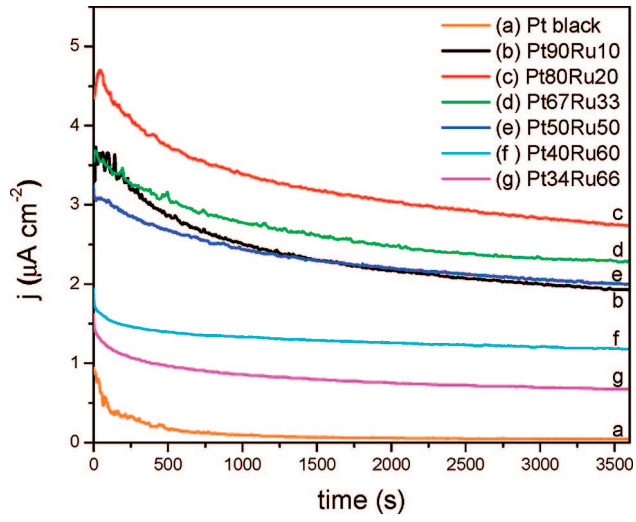

Figure 3. Current density for methanol electrooxidation on Pt/Ru alloy catalysts in 0.5 M methanol + 0.5 M H_2SO_4 at room temperature, up to 1 h. The surface area was normalized from CO stripping experiments.

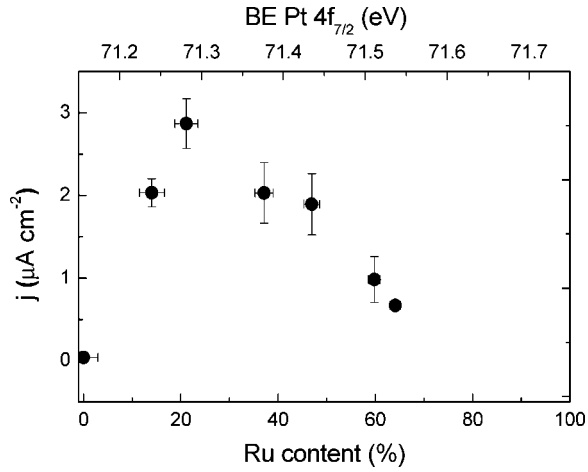

Figure 4. Volcano plot of methanol electrooxidation on Pt/Ru nanoparticles. Uncertainties were calculated from at least three independent measurements.

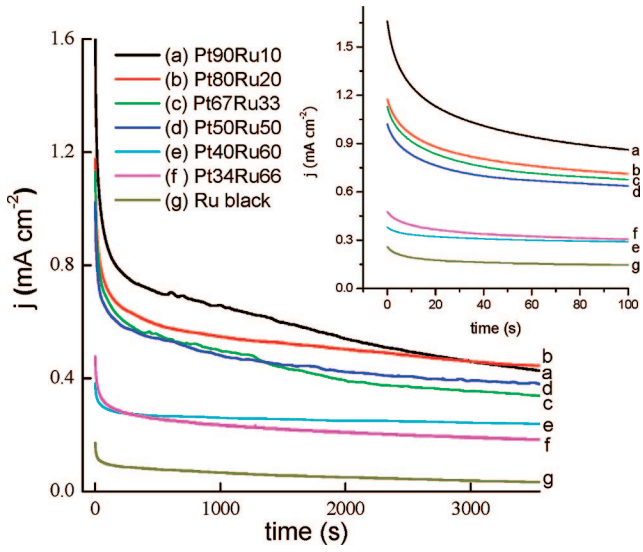

Figure 5. Current−time plots for oxidation of 0.2 M HCOOH in 0.5 M H_2SO_4 recorded at 500 mV vs RHE. The inset shows the current−time data at short reaction time.

20−30% Ru. This behavior cannot be explained by the electronic effect alone. Rather, it proves that the bifunctional mechanism is dominant. For these catalysts, an increase in the Pt $4f_{7/2}$ binding energy would lead to weaker adsorption of the poisoning CO species, and, therefore, reduced poisoning effects. Thus, if the electronic effect was the dominant enhancement mechanism, the reactivity at high CO coverage should also increase with increasing Ru content, in contrast to what is observed (Figure 4). This qualitatively verifies the conclusions made by other groups, including Lu et al.[31] who found that the bifunctional mechanism contributed more significantly than the electronic effect.

The bifunctional mechanism leads to a volcano behavior because of an ensemble effect. It is assumed that an active site consists of the "ensemble" of three Pt atoms and one Ru atom. Gasteiger et al.[9,55] calculated the probability of finding such an ensemble of atoms on the surface of a Pt/Ru catalyst at room temperature, and found that the probability distribution curve peaks at a composition of about 10 atomic % Ru. In Figure 4, the current density peaks at a nominal composition of about 20−30 atomic % Ru. However, for the nanoparticles used in this study, it can be seen in Table 1 that a nominal composition of 20−30 atomic % Ru corresponds to a surface composition of about 17−18 atomic % Ru. The discrepancy between the most active Ru concentration and the peak probability suggests that the bifunctional mechanism is not the only active mechanism. While our data does not allow for the separation of the different mechanisms, our results are in agreement with previous results[9,10,30,31,40] that suggest that the bifunctional mechanism is the primary, but not the only, source of enhancement in the electrooxidation of methanol.

3.3. Formic Acid Electrooxidation on Pt/Ru Nanoparticles. Since the results from electrooxidation of methanol were inconclusive in terms of determining a contribution from an electronic effect (showing predominance of the bifunctional mechanism), electrooxidation of formic acid was next investigated. Formic acid is a promising fuel for study because of its ease of electrooxidation.[6,7,56−61] Decomposition of formic acid has been shown to occur via a triple-pathway mechanism,[41,42] involving a direct pathway to CO_2, an indirect pathway through an adsorbed CO intermediate, and an adsorbed formate intermediate pathway. However, studies have shown that at low potentials (below ~0.6 V vs RHE) and at short reaction times, the direct pathway is dominant on Pt electrodes, and the amount of adsorbed intermediates should be negligible.[33,41] This should provide an opportunity to investigate any possible effects from electronic structure changes separate from the effects of the bifunctional mechanism.

Figure 5 shows the current density for formic acid electrooxidation on the Pt/Ru alloys at 500 mV vs RHE over a period of 1 h. Similar curves were obtained at 450 mV vs RHE. The inset in the figure shows the current density over a period of 100 s. As was the case for methanol electrooxidation, it can be seen that the current density is dependent on the catalyst composition, and that the catalyst is poisoned over time. Based on the known reaction pathways,[33,41,42,62,63] the primary poisoning species is presumed to be CO. The interesting observation, however, arises when the current density is plotted as a function of the catalyst composition (Figure 6a and b). At steady-state (1 h, Figure 6b), a volcano behavior is observed, similar to the behavior for methanol electrooxidation. However, at short reaction times (3 s, Figure 6a), a linear correlation is found, where the instantaneous current density decreases as a function of increasing Ru content.

From the data in Table 1, there appears to be a trend in particle size. It is known that particle size has an effect on the reactivity of a catalyst, largely due to increasing surface area with decreasing size. Both the methanol and formic acid electrooxidation currents were normalized to the surface area of the catalyst, so this effect of particle size should not influence the trends seen in the data. Particle size could still play a part, however, since lattice parameter changes, which are directly connected to binding energy shifts, go along with changes in particle size. As pointed out above, and shown in Table 1, as the particles get smaller, the lattice parameter gets smaller, and the Pt 4f binding energy increases. However, the three samples with the most Ru are all the same size, while the lattice parameters and binding energies continue with the same trends, not connected with particle size. So, while the particle size certainly plays a role in changing the electronic structure of the Pt/Ru catalyst, it does not appear to be the reason for the trends that were observed.

In order to verify the correlation between the current density and the amount of Ru in the catalyst, the turnover frequency[64] (TOF) of Pt active surface sites was calculated, where the TOF is the number of formic acid molecules decomposed to CO_2 per unit time per Pt active site. This calculated value provides

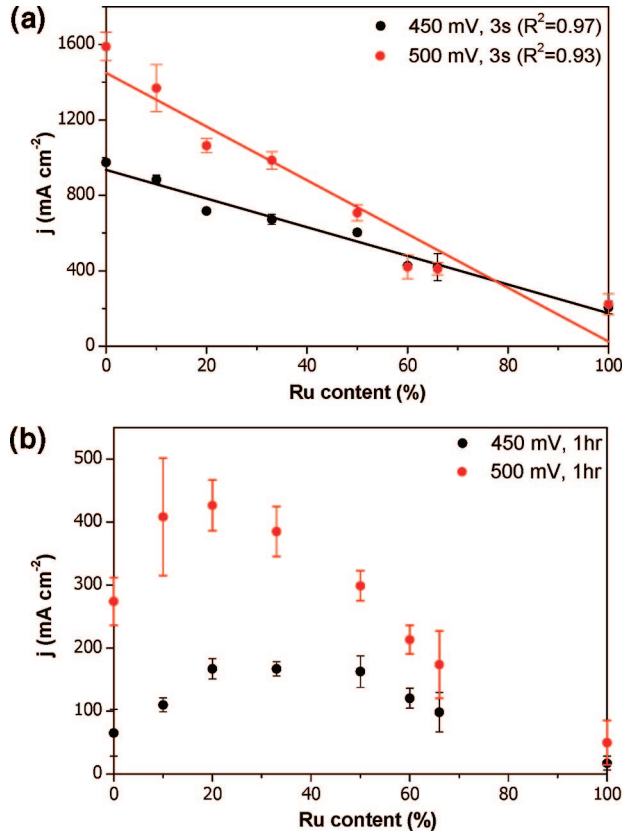

Figure 6. Current density for formic acid electrooxidation at (a) 3 s and (b) 1 h as a function of the Ru amount for Pt/Ru alloy in 0.2 M HCOOH + 0.5 M H_2SO_4 recorded at 450 and 500 mV vs RHE.

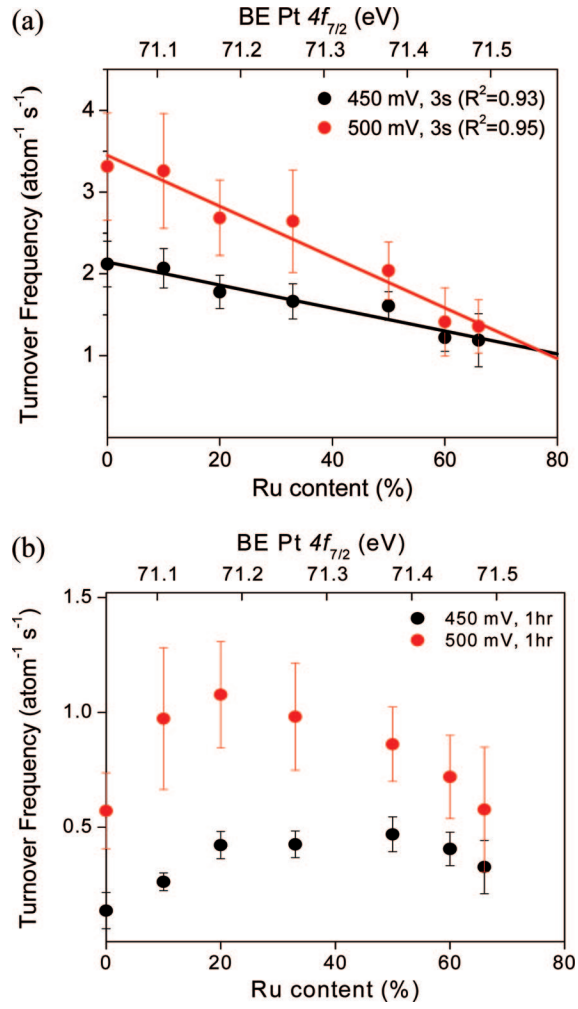

Figure 7. Turnover frequency of Pt sites as a function of the Ru amount and the Pt $4f_{7/2}$ binding energy at (a) 3 s and (b) 1 h. Measurements were done in 0.2 M HCOOH + 0.5 M H_2SO_4 and recorded at 450 and 500 mV vs RHE.

a relative measure of the activity specific to Pt surface atoms by normalizing the current to the number of available active sites. Formic acid is known to decompose on Pt via a dehydration reaction that produces surface CO, which is oxidatively removed at potentials above ~0.4 V vs RHE.[33] Formic acid also decomposes on Ru surfaces.[65−68] However, by comparing the current at 0% and 100% Ru in Figure 6, it is clear that the current on Pt is much greater than that on Ru, which is just above 0 mA cm^{-2} at steady state. While there is some contribution from electrooxidation on Ru, it is very small and should not have a significant effect on the calculation of the TOF of Pt active sites. The surface concentration of Pt active sites for each catalyst, determined with SRPS, see above, is listed in Table 1. In Figure 7a and b, the TOF is plotted as a function of Ru content with the core-level binding energy plotted on the upper *x*-axis. In Figure 7a, the TOF at short reaction times (3 s), where the amount of adsorbed species poisoning the surface is assumed to be negligible, is found to decrease linearly as a function of both increasing Ru content and increasing Pt $4f_{7/2}$ binding energy. As shown in Figure 7b, the TOF at steady-state (1 h) shows a volcano dependence on the Ru amount and Pt $4f_{7/2}$ binding energy.

For these results to be meaningful in terms of the electronic effect, any source of rate-control other than reaction kinetics, namely, mass transport, needs to be excluded as a possible cause of the observed behavior. The contribution of mass transport effects to the reaction rate has been explored previously. In a study of the oxidation of formic acid at platinum and palladized platinum electrodes, Lu et al.[42] demonstrated, using a combination of chronoamperometry and fast cyclic voltammetry, that mass transport is not the rate-limiting step at potentials above 0.45 V. Therefore, we believe that kinetics, rather than mass transport, control the behavior of our catalysts under the conditions used in this work.

In order to be oxidized, formic acid molecules must first be activated at the surface by adsorption. Stronger adsorption of HCOOH results in easier activation, and thus higher reactivity, whereas the opposite is expected for weaker adsorption (of the HCOOH molecule). As already mentioned, Nørskov and coworkers[13] have shown that adsorption energies and activation barriers are correlated to the position of the d-band center with respect to the Fermi level. For the catalysts examined here, the addition of Ru to the catalyst causes the Pt lattice to be compressed, leading to a downshift in the center of gravity of the d-band of Pt with respect to the Fermi level. Since this downshift in the d-band center of Pt results in weaker bonds between the metal surface and the adsorbate, the activation barrier for reaction increases (surface activation of formic acid molecules becomes more difficult). This explains the linear decrease in TOF with increasing Pt $4f_{7/2}$ binding energy, a relationship which confirms the role of the electronic structure in fuel cell electrocatalysis, as predicted by the d-band center theory.

The data for electrooxidation of formic acid at steady-state (after 1 h of reaction) do not give conclusive evidence of the d-band center theory that was provided by the data at short reaction times. At steady-state, the indirect reaction pathways

(through the CO intermediates in the studied potential range[41,63]) are active, complicating the interpretation. The observed behavior, however, is likely due to a combination of the electronic effect and the bifunctional mechanism, as in the case of the methanol study (see above). In addition to the effect of electronic structure on the activation of formic acid molecules, which was demonstrated by the data at short reaction times, there should be an effect on the adsorption strength of CO. As the Ru content and Pt $4f_{7/2}$ binding energy increase, the surface coverage by poisoning intermediates should be reduced, freeing up active surface sites for further electrooxidation of formic acid molecules. This effect would be expected to result in an increase in the TOF with increasing Ru content. Thus, the two effects induced by changes in electronic structure are canceling, not additive. On top of these electronic effects, however, is the bifunctional mechanism. It is well-known that the bifunctional mechanism enhances the oxidative removal of adsorbed CO molecules, and that the enhancement is maximized at a certain composition of Ru due to the ensemble effect[69] (as observed, Figure 6b).

4. Conclusions

This work presents a new approach, involving the use of SRPS, to studying electrocatalysis at bimetallic surfaces that may lead to more detailed insights into the mechanisms of bimetallic systems in fuel cell applications. This study has explored the connection between surface electronic structure and reactivity of small organic molecules as it relates to the d-band center theory proposed by Nørskov and co-workers.[12−19] As the Ru content in Pt/Ru nanoparticles was increased, the binding energy of Pt $4f_{7/2}$ was found to increase linearly, as predicted from the theory. Previous theoretical calculations have indicated that the main reason for the shifts in binding energy in Pt/Ru alloy nanoparticles is lattice strain. Our XRD data give some support to this conclusion, as the Pt lattice was found to compress with the addition of Ru. According to the d-band center theory, compression of the Pt lattice broadens the d-band, and results in a subsequent downshift in energy of the center of the d-band with respect to the Fermi level. In the case of methanol electrooxidation, the production of the strongly adsorbing CO intermediate means that the bifunctional mechanism plays a large role and it is difficult to determine any possible effects of electronic structure changes. Thus, for this system, no conclusive results were obtained regarding a connection between electronic structure and reactivity. On the other hand, this study has demonstrated that it is possible to separate the effects of the electronic structure and the bifunctional mechanism for the case of formic acid electrooxidation by examining the reactivity at different points in time. At steady-state, the turnover frequency of Pt active sites as a function of both the amount of Ru in the catalyst and the Pt $4f_{7/2}$ binding energy was shown to have a volcano behavior, which is likely due to competition between formic acid activation, adsorption strength of reaction intermediates, and the bifunctional mechanism. The data at short reaction times, however, clearly demonstrate the dependence of the reactivity on the electronic structure of the Pt active sites. The turnover frequency was found to decrease linearly with increasing Ru content and increasing Pt $4f_{7/2}$ binding energy. As predicted by the d-band center theory, the downshift in the center of the d-band increases the activation energy of formic acid electrooxidation, and thereby reduces the reactivity.

Acknowledgment. This work is supported by the National Science Foundation under Grant No. NSF CHE06-51083. A.L. acknowledges a partial support from Warsaw University under Grant No. BW-179208. The support by Patrick Hoffmann and Dieter Schmeisser (Brandenburg Technical University Cottbus) in running the beamline U49/2-PGM2 is greatly appreciated. We are indebted to Sascha Hümann and Peter Broekmann (University of Bonn) for their valuable contribution to the cell design, manufacture, and operation of the electrochemical setup at the Bessy-II center at Berlin. We also thank Dr. Scott Wilson, Director of the X-ray Crystallography Laboratory at the University of Illinois, for his assistance with the X-ray crystallographic measurements.

References and Notes

(1) *Handbook of Fuel Cells: Fundamentals, Technology, and Applications*; Vielstich, W.; Lamm, A.; Gasteiger, H. A., Eds.; Wiley: Hoboken, NJ, 2003; Vol. 1−4.
(2) Thomas, S. C.; Ren, X. M.; Gottesfeld, S.; Zelenay, P. *Electrochim. Acta* **2002**, *47*, 3741.
(3) Song, S. Q.; Tsiakaras, P. *Appl. Catal. B* **2006**, *63*, 187.
(4) Antolini, E. *J. Power Sources* **2007**, *170*, 1.
(5) Spendelow, J. S.; Wieckowski, A. *Phys. Chem. Chem. Phys.* **2007**, *9*, 2654.
(6) Rice, C.; Ha, R. I.; Masel, R. I.; Waszczuk, P.; Wieckowski, A.; Barnard, T. *J. Power Sources* **2002**, *111*, 83.
(7) Rice, C.; Ha, S.; Masel, R. I.; Wieckowski, A. *J. Power Sources* **2003**, *115*, 229.
(8) Petrii, O. A. *J. Solid State Electrochem.* **2008**, *12*, 609.
(9) Gasteiger, H. A.; Markovic, N.; Ross, P. N.; Cairns, E. J. *J. Phys. Chem.* **1993**, *97*, 12020.
(10) Yajima, T.; Uchida, H.; Watanabe, M. *J. Phys. Chem. B* **2004**, *108*, 2654.
(11) Rodriguez, J. A.; Goodman, D. W. *Science* **1992**, *257*, 897.
(12) Kitchin, J. R.; Nørskov, J. K.; Barteau, M. A.; Chen, J. G. *Phys. Rev. Lett.* **2004**, *93*, 156801.
(13) Hammer, B.; Nørskov, J. K. *Surf. Sci.* **1995**, *343*, 211.
(14) Hammer, B.; Hansen, L. B.; Nørskov, J. K. *Phys. Rev. B* **1999**, *59*, 7413.
(15) Hammer, B.; Morikawa, Y.; Nørskov, J. K. *Phys. Rev. Lett.* **1996**, *76*, 2141.
(16) Hammer, B.; Nielsen, O. H.; Nørskov, J. K. *Catal. Lett.* **1997**, *46*, 31.
(17) Hammer, B.; Nørskov, J. K. Theoretical surface science and catalysis - Calculations and concepts. In. *Adv. Catal.* **2000**, *45*, 71.
(18) Nørskov, J. K.; Bligaard, T.; Logadottir, A.; Bahn, S.; Hansen, L. B.; Bollinger, M.; Bengaard, H.; Hammer, B.; Sljivancanin, Z.; Mavrikakis, M.; Xu, Y.; Dahl, S.; Jacobsen, C. J. H. *J. Catal.* **2002**, *209*, 275.
(19) *Chemical Bonding at Surfaces and Interfaces*; 1st ed; Nilsson, A.; Pettersson, L. G. M.; Nørskov, J. K., Eds.; Elsevier: Amsterdam, The Netherlands, 2008; p 533.
(20) Nørskov, J. K. *Rep. Prog. Phys.* **1990**, *53*, 1253.
(21) Kibler, L. A.; El-Aziz, A. M.; Hoyer, R.; Kolb, D. M. *Angew. Chem., Int. Ed.* **2005**, *44*, 2080.
(22) Mavrikakis, M.; Hammer, B.; Nørskov, J. K. *Phys. Rev. Lett.* **1998**, *81*, 2819.
(23) Richter, B.; Kuhlenbeck, H.; Freund, H. J.; Bagus, P. S. *Phys. Rev. Lett.* **2004**, *93*, 026805.
(24) Rodriguez, J. A. *Surf. Sci. Rep.* **1996**, *24*, 225.
(25) Bagus, P. S.; Illas, F.; Pacchioni, G.; Parmigiani, F. *J. Electron Spectrosc. Relat. Phenom.* **1999**, *100*, 215.
(26) Bagus, P. S.; Wieckowski, A.; Freund, H. *Chem. Phys. Lett.* **2006**, *420*, 42.
(27) Weinert, M.; Watson, R. E. *Phys. Rev. B* **1995**, *51*, 17168.
(28) Lu, C.; Lee, I. C.; Masel, R. I.; Wieckowski, A.; Rice, C. *J. Phys. Chem. A* **2002**, *106*, 3084.
(29) Tong, Y. Y.; Kim, H. S.; Babu, P. K.; Waszczuk, P.; Wieckowski, A.; Oldfield, E. *J. Am. Chem. Soc.* **2002**, *124*, 468.
(30) Waszczuk, P.; Lu, G. Q.; Wieckowski, A.; Lu, C.; Rice, C.; Masel, R. I. *Electrochim. Acta* **2002**, *47*, 3637.
(31) Lu, C.; Rice, C.; Masel, R. I.; Babu, P. K.; Waszczuk, P.; Kim, H. S.; Oldfield, E.; Wieckowski, A. *J. Phys. Chem. B* **2002**, *106*, 9581.
(32) Alayoglu, S.; Nilekar, A. U.; Mavrikakis, M.; Eichhorn, B. *Nat. Mater.* **2008**, *7*, 333.
(33) Markovic, N. M.; Gasteiger, H. A.; Ross, P. N.; Jiang, X. D.; Villegas, I.; Weaver, M. J. *Electrochim. Acta* **1995**, *40*, 91.
(34) Markovic, N. M.; Ross, P. N. *Surf. Sci. Rep.* **2002**, *45*, 121.
(35) Watanabe, M.; Zhu, Y. M.; Igarashi, H.; Uchida, H. *Electrochemistry* **2000**, *68*, 244.
(36) Zhou, W. P.; Lewera, A.; Larsen, R.; Masel, R. I.; Bagus, P. S.; Wieckowski, A. *J. Phys. Chem. B* **2006**, *110*, 13393.

(37) Zhou, W. P.; Lewera, A.; Bagus, P. S.; Wieckowski, A. *J. Phys. Chem. C* **2007**, *111*, 13490.
(38) Lewera, A.; Zhou, W. P.; Vericat, C.; Chung, J. H.; Haasch, R.; Wieckowski, A.; Bagus, P. S. *Electrochim. Acta* **2006**, *51*, 3950.
(39) Chrzanowski, W.; Kim, H.; Wieckowski, A. *Catal. Lett.* **1998**, *50*, 69.
(40) Kardash, D.; Korzeniewski, C.; Markovic, N. *J. Electroanal. Chem.* **2001**, *500*, 518.
(41) Chen, Y. X.; Heinen, M.; Jusys, Z.; Behm, R. B. *Angew. Chem., Int. Ed.* **2006**, *45*, 981.
(42) Lu, G. Q.; Crown, A.; Wieckowski, A. *J. Phys. Chem. B* **1999**, *103*, 9700.
(43) Herrero, E.; Chrzanowski, W.; Wieckowski, A. *J. Phys. Chem.* **1995**, *99*, 10423.
(44) Lewera, A.; Zhou, W. P.; Hunger, R.; Jaegermann, W.; Wieckowski, A.; Yockel, S.; Bagus, P. S. *Chem. Phys. Lett.* **2007**, *447*, 39.
(45) Hennig, D.; Ganduglia-Pirovano, M. V.; Scheffler, M. *Phys. Rev. B* **1996**, *53*, 10344.
(46) Vericat, C.; Wakisaka, M.; Haasch, R.; Bagus, P. S.; Wieckowski, A. *J. Solid State Electrochem.* **2004**, *8*, 794.
(47) Seah, M. P. *Surf. Interface Anal.* **1980**, *2*, 222.
(48) Tanuma, S. In *Surface Analysis by Auger and X-ray Photoelectron Spectroscopy*; Briggs, D., Grant, J. T., Eds.; IM Publications and Surface Spectra Limited: Charlton, Chichester, West Sussex, 2003.
(49) Babu, P. K.; Kim, H. S.; Oldfield, E.; Wieckowski, A. *J. Phys. Chem. B* **2003**, *107*, 7595.
(50) Rose, A.; Crabb, E. M.; Qian, Y. D.; Ravikumar, M. K.; Wells, P. P.; Wiltshire, R. J. K.; Yao, J.; Bilsborrow, R.; Mosselmans, F.; Russell, A. E. *Electrochim. Acta* **2007**, *52*, 5556.
(51) Han, B. C.; Van der Ven, A.; Ceder, G.; Hwang, B. J. *Phys. Rev. B* **2005**, *72*, 205409.
(52) Cao, D.; Lu, G. Q.; Wieckowski, A.; Wasileski, S. A.; Neurock, M. *J. Phys. Chem. B* **2005**, *109*, 11622.
(53) Balandin, A. A. *Adv. Catal.* **1958**, *10*, 96.
(54) Ichikawa, S. *Chem. Eng. Sci.* **1990**, *45*, 529.
(55) Gasteiger, H. A.; Markovic, N.; Ross, P. N.; Cairns, E. J. *J. Electrochem. Soc.* **1994**, *141*, 1795.
(56) Zhao, M. C.; Rice, C.; Masel, R. I.; Waszczuk, P.; Wieckowski, A. *J. Electrochem. Soc.* **2004**, *151*, A131.
(57) Waszczuk, P.; Barnard, T. M.; Rice, C.; Masel, R. I.; Wieckowski, A. *Electrochem. Commun.* **2002**, *4*, 599.
(58) Ha, S.; Dunbar, Z.; Masel, R. I. *J. Power Sources* **2006**, *158*, 129.
(59) Larsen, R.; Ha, S.; Zakzeski, J.; Masel, R. I. *J. Power Sources* **2006**, *157*, 78.
(60) Ha, S.; Larsen, R.; Masel, R. I. *J. Power Sources* **2005**, *144*, 28.
(61) Zhu, Y. M.; Ha, S. Y.; Masel, R. I. *J. Power Sources* **2004**, *130*, 8.
(62) Chen, Y. X.; Heinen, M.; Jusys, Z.; Behm, R. J. *Langmuir* **2006**, *22*, 10399.
(63) Chen, Y. X.; Ye, S.; Heinen, M.; Jusys, Z.; Osawa, M.; Behm, R. J. *J. Phys. Chem. B* **2006**, *110*, 9534.
(64) Somorjai, G. A. *Introduction to surface chemistry and catalysis*; Wiley: New York, 1994.
(65) Barros, R. B.; Garcia, A. R.; Ilharco, L. M. *Surf. Sci.* **2005**, *591*, 142.
(66) Lei, T.; Lee, J.; Zei, M. S.; Ertl, G. *J. Electroanal. Chem.* **2003**, *554−555*, 41.
(67) Meng, B.; Jachimowski, T. A.; Sun, Y.; Weinberg, W. H. *Surf. Sci.* **1994**, *315*, L959.
(68) Sun, Y. K.; Weinberg, W. H. *J. Chem. Phys.* **1991**, *94*, 4587.
(69) Gasteiger, H. A.; Markovic, N.; Ross, P. N.; Cairns, E. J. *J. Phys. Chem.* **1994**, *98*, 617.

JP805374P